Research

iMedPub Journals
www.imedpub.com

Nano Research & Applications
ISSN 2471-9838

2022
Vol.8 No.9:95

In-Situ Synthesis of Nanostructured Tio_2-Zns Composite with Enhanced Photocatalytic Activity

Srikrishna Samanta, Hasmat Khan, Malobi Seth and Sunirmal Jana*

Department of Specialty Glass Division, CSIR-Central Glass and Ceramic Research Institute, West Bengal, India

***Corresponding author:** Sunirmal Jana, Department of Specialty Glass Division, CSIR-Central Glass and Ceramic Research Institute, West Bengal, India, Email: sjana@cgcri.res.in

Received date: August 05, 2022, Manuscript No. Ipnto-22-14125; **Editor assigned date:** August 08, 2022, PreQC No. Ipnto-22-14125 (PQ); **Reviewed date:** August 17, 2022, QC No. Ipnto-22-14125; **Revised date:** August 24, 2022, Manuscript No. Ipnto-22-14125 (R); **Published date:** September 05, 2022, DOI: 10.36648/2471-9838.8.9.91

Citation: Samanta S, Khan H, Seth M, Jana S (2022) *In-Situ* Synthesis of Nanostructured Tio_2-Zns Composite with Enhanced Photocatalytic Activity. Nano Res Appl Vol.8 No.9: 91.

Abstract

For the first time, we report the single step in-situ synthesis of hierarchical TiO_2-ZnS nanostructure (TiO_2 sphere wrapped with ZnS nanorods) for photocatalytic degradation of rhodamine B under UV light irradiation. In the typical synthesis, titanium oxysulfate and zinc nitrate hexahydrate were used as precursor materials for TiO_2 and ZnS, respectively whereas dimethyl formamide and distilled water used as solvents. The content of ZnS and TiO_2 in TiO_2-ZnS composite was controlled by tuning the concentration of respective precursor materials in the solution. As-synthesize materials was centrifuged and washed with distilled water several times. Finally, the sample was cured at 500°C in an electrical furnace under air atmosphere. Morphology and microstructure of the synthesized materials were characterized by field emission scanning electron and transmission electron microscopes. Crystallinity and structural properties were investigated with the help of X-ray diffraction study. X-ray photoelectron spectroscopic characterization was performed to observe the oxidation states of the constituent elements present in the sample. Moreover, the optical properties of the samples were analyzed systematically. Finally, all the materials and optical properties were correlated with the photocatalytic activity of the materials. It was noted that hierarchical structured TiO_2-ZnS sample showed around 1.5 times higher photocatalytic activity towards rhodamine B degradation compared to pristine TiO_2 under UV light irradiation. This work could make an avenue for the synthesis of other multicomponent efficient photocatalyst.

Keywords: Solvothermal method; *In-situ* synthesis; TiO_2-ZnS hierarchical nanostructure; Photocatalytic activity

Introduction

Rapid growth of organic dye-manufacturing and dye-consuming industries which generate wastewaters always draws a special attention to the materials researchers due to the serious environmental concern [1-3]. Generally, organic-dyes are intractable compounds that are very hard to remove by biological treatment [2-4]. However, the nanostructured Metal Oxide Semiconductor (MOS) as photocatalyst could efficiently and economically eliminate such toxic organic compounds by decomposing into the less toxic materials like CO_2 and water [5]. In photocatalysis, highly reactive oxygen species such as hydroxyl and superoxide radicals are generated to react with dyes and decompose them in the presence of a semiconductor and ultraviolet or visible light [5-7]. Among the various MOS, titanium dioxide has been extensively studied over the past few decades due to its potential applications in different fields. From the first discovery of hydrogen production by TiO_2 photoanode under UV irradiation, lots of research on TiO_2 has been performed, which has broadly expanded the applications of TiO_2 in the various fields like photovoltaic cells, dye-sensitized solar cells, photocatalysis, environmental remediation as well as photoelectrochemical sensors [4,5]. Moreover, TiO_2 is widely used as photocatalysts for removal of hazardous organic compounds as well as the self-cleaning environmental applications due to its strong oxidizing and reducing ability under UV light, relatively high efficiency, low cost and availability [8]. The photocatalytic activity of TiO_2 is improved by increasing surface area which provides more active sites for photocatalytic reactions. In this regard, nanostructuring of MOS is the renowned method to increase the surface area of the materials [9,10]. Da Silva et al. [11] reported Wulff-shape mesoporous TiO_2 for enhanced photocatalytic activity. Liu et al. [12] also reported spindle-shaped mesoporous TiO_2 as a superior photocatalyst.

However, rapid photogenerated charge carrier recombination in TiO_2 limits its photocatalytic efficiency. Metal doping and coupling of TiO_2 with other suitable semiconducting metal oxides/sulphides are widely used approaches to improve the photogenerated charge separation and photocatalytic activity [11-14]. In this regard, semiconducting metal sulphides especially ZnS has been broadly studied due to its environmental friendliness and earth abundance [15]. ZnS is an important semiconductor material having a wide direct optical band gap of 3.6 eV [16]. Only UV light is required to promote excited electrons to the conduction band of ZnS [16,17]. This type of material with high band gap energy may act as a good electron trapper due to its vacant conduction band [12]. Moreover, coupling of TiO_2 with ZnS enhances the photocatalytic activity of

the nanocomposite compared to pristine TiO_2 and pristine ZnS by forming type-II heterojunction between TiO_2 and ZnS [13]. In this regard, Vaclav et al. [14] synthesized TiO_2/ZnS nanocomposite and reported better photocatalytic activity compared to bare TiO_2 and ZnS nanoparticles. Moreover, Xiaodan et al. [18] prepared ZnS/TiO_2 nanocubes *via* solvothermal method showed the enhanced photocatalytic activity of the composite compared to pristine anatase TiO_2 under visible light exposure. Franco et al. [19] also synthesized nanocrystalline TiO_2-capped ZnS *via* chemical vapor deposition technique and reported the increased photoactivity of TiO_2-capped ZnS compared to bare TiO_2. However, most of the reports available in the literatures are related to the two steps synthesis of TiO_2-ZnS nanocomposite which is time consuming and relatively high cost [20-22]. To the best of our knowledge, there are no reports available on single step in-situ synthesis of hierarchical TiO_2-ZnS nanostructure (TiO_2 sphere wrapped with ZnS nanorods) in the literatures.

In this work, titanium oxysulfate and zinc nitrate hexahydrate were used as precursor materials for TiO_2 and ZnS, respectively whereas DMF and distilled water as solvents. The reaction mixture was transferred into a 150 ml Teflon-lined stainless steels autoclave and kept in an oven at 150°C for 6 hours. The precipitate was cooled down to room temperature and washed several times with distilled water. Then, the sample was cured at 500°C for 2 hours in an electrical furnace. Pure TiO_2 was synthesized with the same procedure as adopted for TiO_2-ZnS composite using titanium oxysulfate as a precursor for comparison. Finally, structural, materials and optical properties of the synthesize materials were correlated with the photocatalytic activity.

Experiment

Precursor materials

Zinc nitrate hexahydrate (ZN, Merck, 97% purity), Titanium oxysulfate (TIOS, Sigma Aldrich, 99% purity), DMF (Merck, 98% purity) and Distilled water.

Synthesis of hierarchical TiO_2-ZnS nanostructure

For the preparation of TiO_2-ZnS nanostructure (TZS), 1.10 g Zn $(NO_3)_2.6H_2O$ (3 mmol), 2.64 g TiO $(SO_4)_2$ (7 mmol) were taken in 85 ml DMF followed by the addition of 5 ml H_2O and the resultant mixture was stirred for 30 min. Then the turbid solution was stirred and heated on a magnetic stirrer at 90°C to obtain clear homogeneous solution. The resultant clear solution was cooled down to room temperature and then poured it into a 150 ml Teflon-lined stainless-steel autoclave and kept in an oven at 150°C for 6 hours. The precipitate was cooled down to room temperature and washed several times with distilled water. Finally, the sample was cured at 500°C for 2 hours in an electrical furnace. Pure TiO_2 was synthesized with the same procedure as adopted for TiO_2-ZnS composite using titanium oxysulfate as a precursor material.

Characterization

X-Ray Diffraction (XRD) study of the sample was performed by Rigaku Smart Lab using CuKa radiation (1.5406°A) operating at 9 kW in the diffraction angle (2θ), 20 to 800. The surface morphology of the materials was investigated by FESEM (ZEISS, SUPRA™35VP) study. TEM measurements were carried out by Tecnai G2 30ST (FEI) electron microscope operating at 300 kV from the dispersed material by ultrasonication onto 300 mesh carbon coated cupper grid. TEM/HRTEM and TEM-EDS were performed to analyses the particle size, crystal phase and content of elements. UV-Vis-NIR spectrophotometer (Shimadzu UV-PC-3100; photometric accuracy: transmission ± 0.3%, wavelength resolution, 0.10 nm) was used to measure UV-Vis absorption spectra of the sample. Band Gap Energy (BGE) of the samples was calculated from the respective absorption spectrum. PerkinElmer (LS55) spectrofluorometer was employed to measure the photoluminescence property of the sample at room temperature. X-ray Photoelectron Spectra (XPS) of the sample was done by employing PHI Versaprobe II Scanning XPS microprobe surface analysis system using Al-Ka X-rays (hn, 1486.6 eV; DE, 0.7 eV at room temperature). The energy scale of the spectrometer was calibrated with pure (Ag) samples and the pressure in the XPS analysis chamber was better than 5×10^{-10} mbar. The chemical state of each element present in the nanocomposite was determined by taking position of (C1s) peak as standard (with the binding energy of 284.5 eV).

Measurement of photocatalytic activity

Photocatalytic Activity (PA) of the nanocomposite towards degradation of Rhodamine B (Rh-B) was studied in a custom-built stainless-steel UV (wavelength, 254 nm) curing chamber. The total solution in 5 ml capacity cuvate containing the solution of dye (10^{-5} M, Co) was placed in UV chamber. The detailed PA measurement set up has already been reported anywhere [19-22]. The PA of the synthesized materials was performed under UV light irradiation. For this purpose, a 300 W high-pressure xenon lamp (PLSSXE300UV, Beijing Trust tech. Co. Ltd., wavelength ranges from 300 to 800 nm with total intensity of ca. 200 mW/cm^2) have been used to carry out the experiment. For this experiment,~ 5 ml dye solution took out a certain time of interval and UV-visible absorption spectrum was recorded to finish the remnant Concentration (C) of the dye with the help of a calibration curve of the dye solutions. The calibration curve was drawn by plotting dye concentration against absorbance at 554 nm peak wavelength of Rh-B solutions obeying Lambert Bayer's law. The PA of the catalyst was analysed by plotting ln (Co/C) (dye concentration; Co, initial and C, remnant) versus irradiation time. The rate constants of decomposition reaction (considering pseudo first order reaction kinetics) were calculated from the plots.

Results and discussion

Phase structure

The X-ray diffraction patterns (Figure 1) of the samples were recorded in the 2θ range 20° to 80° to investigate the

crystallinity and crystal phase of TiO_2 and ZnS. From the X-ray diffraction peaks it was found that both the TiO_2 and ZnS in the TZS sample crystalizes as anatase TiO_2 and cubic ZnS, respectively. The diffraction peaks (2θ degree) centered at 25°, 38°, 48°, 54°, 63° and 75° corresponded to the (101), (112), (200), (105), (204) and (215), respectively confirms the anatase phase of TiO_2 (JCPDS card no. 21-1272). Moreover, the diffraction peaks (2Θ) located at 28° and 56° corresponded to the (111) and (311) planes arise mainly due to the formation of cubic ZnS (JCPDS card no. 05-0566) in TZS sample. The crystallite size of the samples was calculated with the help of Debye-Scherrer's equation (eqn. 1) [14].

$$D = \frac{k\lambda}{\beta \cos\theta} \quad \text{----- (1)}$$

Where, k is proportionality constant (0.9), λ is wavelength of X-ray (1.5406 Å), β denoted as FWHM (Full Width at Half Maximum) of the peak of maximum intensity in radians, Θ is diffraction angle and D is crystallite size.

It was found that the calculated average crystallite size (D) of pristine TiO_2 was ~ 52 nm whereas the same for TiO_2 and ZnS were ~ 43 nm and ~ 36 nm, respectively in TZS sample.

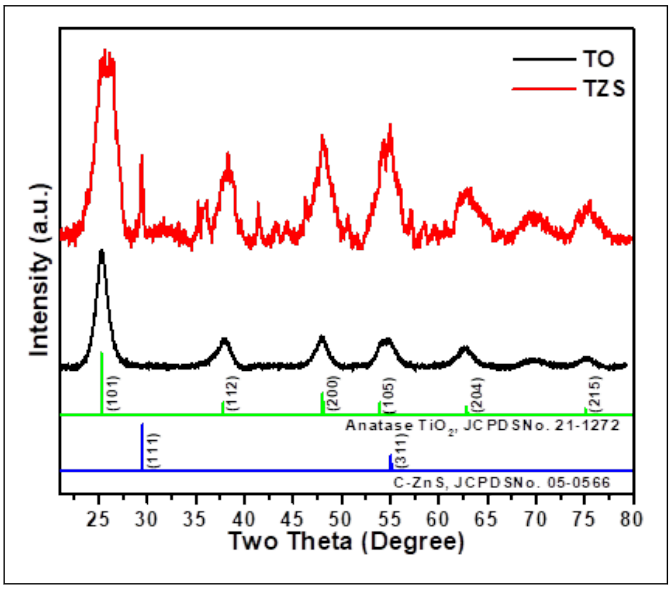

Figure 1: XRD patterns of pristine TiO_2 (TO) and TiO_2-ZnS (TZS) samples.

Morphology and Microstructure

FESEM Study

Surface morphology of the synthesized pristine TiO_2 and TZS samples were analysed with the help of FESEM study (Figure 2).

The samples were synthesized by solvothermal technique followed by curing at 500°C under air atmosphere to obtain the hierarchical sphere like morphology. The FESEM image shows the formation of spherical TiO_2. Size of TiO_2 spheres was calculated from the FESEM image and it was in the range of ~ 0.9 to ~ 2.0 µm. It is seemed to be appeared the hierarchical sphere like morphology of the TZS sample after changing the amount of precursor solutions in the reaction mixture. It was found that the TiO_2 spheres were uniformly wrapped with ZnS nanorods at a particular solution composition (Ti: Zn = 7:3, mol ratio) whereas at the other solution compositions (Ti: Zn = 8:2, and Ti: Zn = 6:4, mol ratio), ZnS nanorods were found to be sparsely distributed on the surface of the TiO_2 spheres. Length and width of the ZnS nanorods were also calculated from the FESEM image these were ~ 400 nm and ~ 60 nm, respectively. TiO_2 spheres wrapped with ZnS nanorods in TZS sample would be beneficial to improve the photocatalytic activity of the sample.

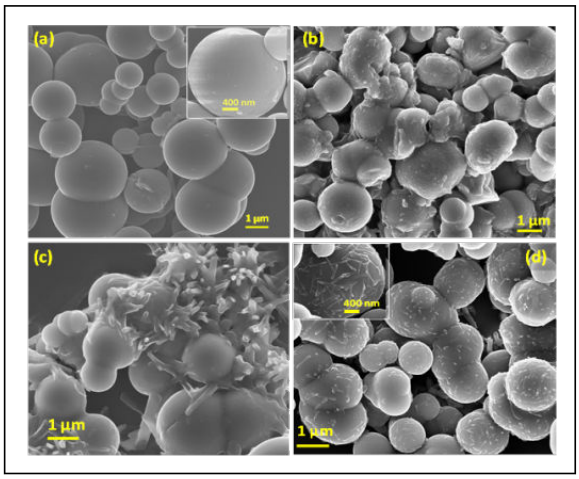

Figure 2: FESEM images of the samples synthesized *via* solvothermal technique by tuning the precursor solutions composition: (a) pristine TiO_2 (b) TZS (Ti: Zn = 8:2, mol ratio) (c) TZS (Ti: Zn = 6:4, mol ratio) and (d) TZS (Ti: Zn = 7:3, mol ratio). Insets of (a) and (d) represents the higher magnified FESEM images.

TEM study

The microstructural properties of TZS sample was investigated by TEM study (Figure 3). Figure 3a, b show the bright field TEM images of the sample. From the bright field TEM images, it is clearly seen that the TiO_2 spheres are wrapped with ZnS nanorods. This observation was further confirmed from the FESEM images of the sample. It was confirmed from the HRTEM image that the sample was fully crystallised with anatase TiO_2 (a-TiO_2) and cubic ZnS (c-ZnS) at the experimental curing temperature of 500°C [5]. This observation was further confirmed from XRD study. Moreover, the TEM EDS plot showed the presence of titanium, zinc, sulphur and oxygen elements in the sample.

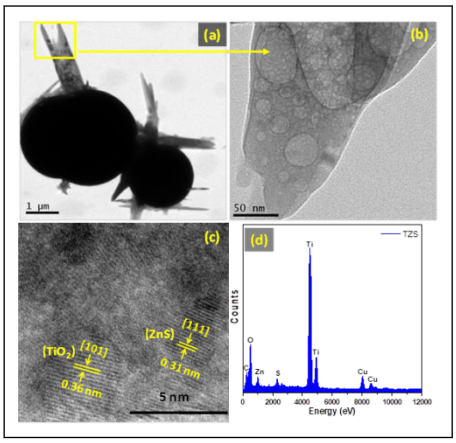

Figure 3: TEM microstructural studies of TZS sample cured at 500°C: (a-b) Bright field TEM images, (c) HRTEM image and (d) EDS plot.

XPS Study

The XPS analysis was performed to observe the oxidation states of the constitute elements present in TZS sample. The strong binding energy peaks (Figure 4) centered at 1044.2 eV and 1021.3 eV, corresponded to the core levels of Zn2p1/2 and Zn2p3/2, respectively confirmed the presence of Zn^{2+} ions in the sample [23,24]. Figure 4b shows the binding energy curve of Ti2p with two intense peaks located at ~ 458.5 eV and 464.4 eV, corresponded to core levels of Ti2p3/2 and Ti2p1/2, respectively. The binding energy difference between the two peaks was calculated and found to be ~ 5.9 eV, confirmed the existence of Ti^{4+} in the TZS sample [10]. Figure 4c shows the broad binding energy peaks of O1s. The broad nature of the O1s peak could indicate the presence of Olattice, Odefect (surface oxygen vacancies) and Ohydroxyl [17]. The presence of oxygen defects in the sample could help to improve the photocatalytic activity by enhancing light absorption [18]. Moreover, the presence of sulphur ion in the sample was confirmed from the binding energy peak centered at 163.7 eV (S2p1/2) and 161.8 eV (S2p3/2) corresponded to the S-interstitial state and S2-, respectively [25].

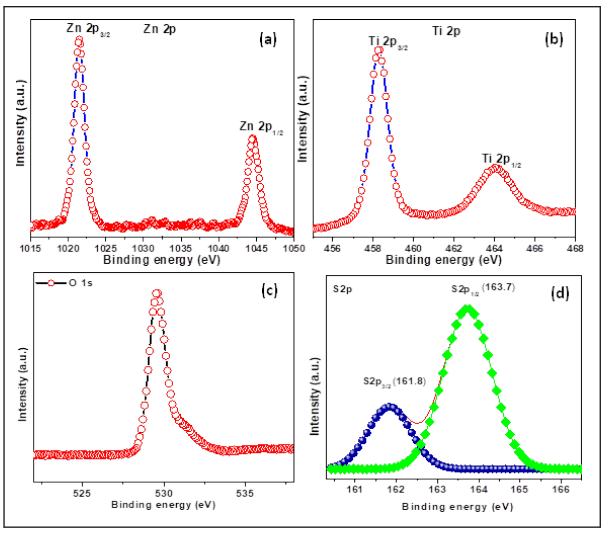

Figure 4: XPS biding energy curves of TZS sample: (a) Zn2p, (b) Ti2p, (c) O1s and (d) S2p.

Photo Luminescence (PL) study

The PL spectral study of pristine TiO_2 and TZS samples was performed and shown in Figure 5. The PL spectra of pristine TiO_2 and TiO_2-ZnS nanocomposites were recorded at an excitation wavelength of 325 nm. The PL spectra of both TiO_2 and TZS exhibit a strong emission peak centered at ~ 397 nm which could be ascribed to the band edge emission of anatase TiO_2 semiconductor [26]. The presence of a sharp emission peak centered at 425 nm can be recognized to the recombination of self-trapped excitons in anatase TiO_2 [27]. The shoulder peaks centered at 451 and 468 nm are related to the transition of an electron from the shallow level of oxygen vacancies to the valence band [27]. Moreover, a broad and intense peak at 486 nm appeared due to the presence of Ti^{4+} ions adjacent to oxygen vacancies (intra gap surface states) [28]. On the other hand, TZS nanocomposite exhibited a weak emission peak at 397 nm compared to pristine TiO_2 due to the interaction between TiO_2 and ZnS [27]. This interaction could facilitate the photogenerated charge carrier separation vis-à-vis enhance the photocatalytic activity [27].

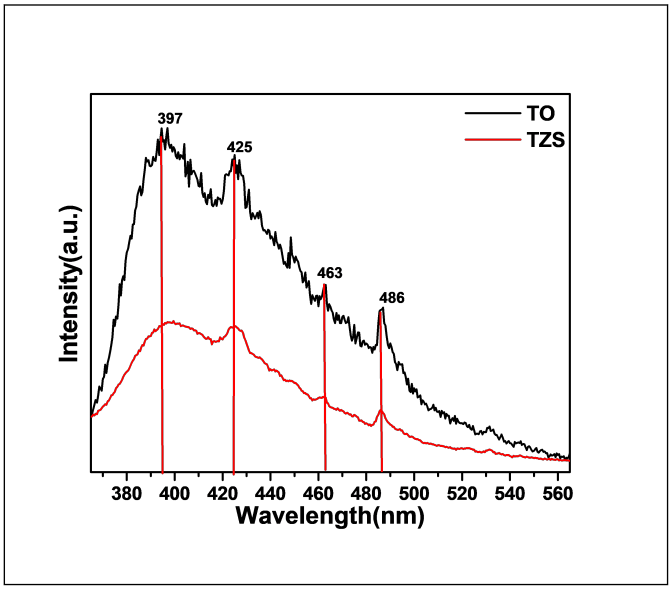

Figure 5: PL spectra of TiO_2 and TZS nanocomposites.

UV-Visible absorption study

The optical properties of the samples were characterized with the help of UV-Vis spectrophotometer and shown in Figure 6. It was found that the anatase TiO_2 exhibited a wide absorption band in the range from 200 to 385 nm whereas TiO_2-ZnS composite showed a UV absorption band in the range from 200 to 338 nm. The UV-Vis spectrum of TiO_2-ZnS composite showed blue shift compared to pristine TiO_2. This observation could be attributed to the interaction of ZnS with TiO2 [17,18,29]. The optical band gap energies of the samples were estimated from the corresponding absorption spectra using Tauc equation [22]. It was noted that the calculated band gap energies are ~3.3 ± 0.03 and 3.56 ± 0.01 eV for pristine TiO_2 and TiO_2-ZnS nanocomposite, respectively. The widening of the band gap

energy in the TiO_2-ZnS composite compared to pristine TiO_2 beneficiates the efficient charge separation vis-a-vis improved photocatalytic activity [18,29].

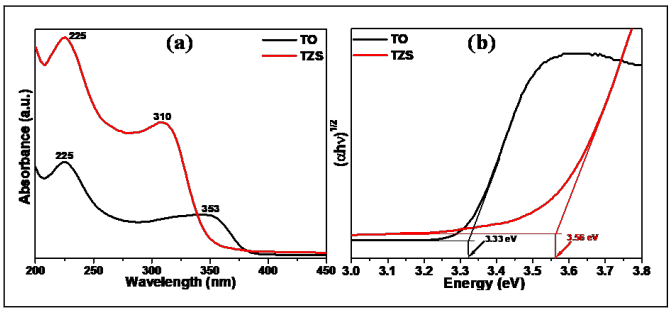

Figure 6: UV-Vis absorption and optical band gap energy of pristine TiO_2 and TiO_2-ZnS composites.

Photocatalytic Performance

Photocatalytic Activity (PA) of pristine TiO_2 (TO) and TZS composite was evaluated by measuring of organic dye (Rhodamine B, RhB) degradation under UV light irradiation. The PA of synthesized samples was examined by the degradation of organic pollutants (RhB) as a function of time. It was noted that the reduction of concentration of the RhB was measured from the relative intensity of characteristic peak at 554 nm from the UV absorbance spectra. The time dependent UV absorption spectra (Figure 7) of TO and TZS shows the decomposition of RhB with irradiation time of 50 min. Under the UV irradiation time of 50 min the TZS sample almost decomposed the RhB dye. The TZS composite exhibited higher PA compared to TO. This observation could be attributed to the formation of heterojunction between TiO_2 and ZnS [30]. The photocatalytic reduction rate of the samples can be designated by pseudo-first-order kinetics. So, the plots of ln (C0/Ct) versus irradiation time were examined. It was found that the ln (C0/Ct) curves versus irradiation time were linear, suggested pseudo first-order kinetics [5]. The rate constant K was calculated and it was found 0.0175 min^{-1} and 0.0241 min^{-1} for TO and TZS composite, respectively. The K value for the TZS sample was ~1.5 times higher than that of TO. Thus, it is concluded that the presence of ZnS onto the TiO_2 surface resulted the improved PA towards photocatalytic organic dye degradation under UV light irradiation.

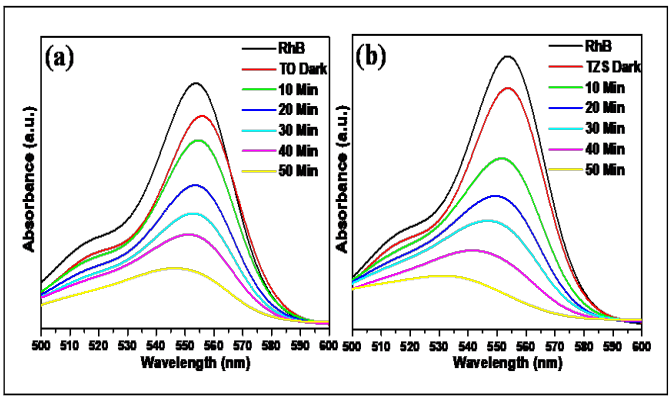

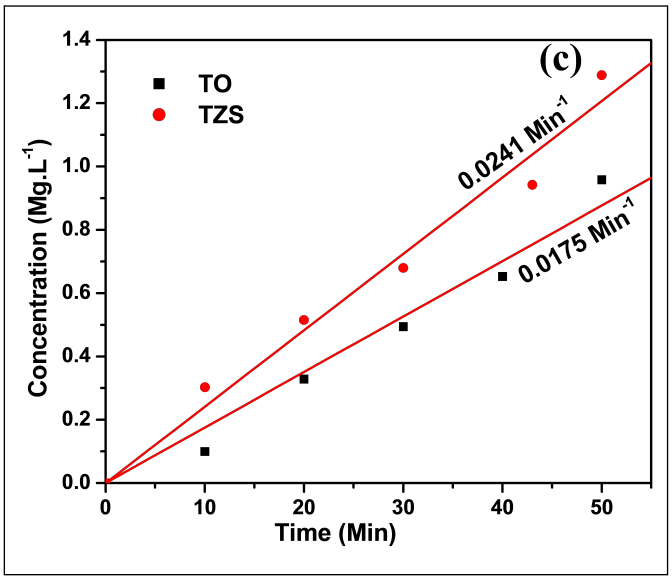

Figure 7: UV absorption spectra for photocatalytic dye degradation (a,b) and rate constant curves of rhodamine B (c) for pristine TiO_2 and TiO_2-ZnS nanocomposites.

Conclusions

For the first time, we successfully synthesize the hierarchical TiO_2-ZnS nanostructure (TiO_2 sphere wrapped with ZnS nanorods) by single step solvothermal process for photocatalytic degradation of rhodamine B under UV light irradiation. Titanium oxysulfate and zinc nitrate hexahydrate were used as precursor materials for TiO_2 and ZnS, respectively whereas DMF and distilled water as solvents. The reaction mixture was transferred into a 150 ml Teflon-lined stainless steels autoclave and kept in an oven at 150°C for 6 hours. The precipitate was cooled down to room temperature and washed several times with distilled water. Then, the sample was cured at 500°C for 2 hours in an electrical furnace. Pure TiO_2 was synthesized with the same procedure as adopted for TiO_2-ZnS composite using titanium oxysulphate as a precursor for comparison. Finally, structural, materials and optical properties of the synthesize materials were correlated with the photocatalytic activity. It was noted that hierarchical TiO_2-ZnS sample showed around 1.5 times higher photocatalytic activity towards rhodamine B degradation compared to pristine TiO_2 under UV light irradiation. This work could make an avenue for the synthesis of other multicomponent efficient photocatalyst for environmental remediation.

Acknowledgement

The authors are grateful to Director, CSIR-CGCRI, Kolkata for his kind support and encouragement. The authors also acknowledge the help rendered by Nanostructured Materials Division and Electron Microscopy Section for microstructural characterizations. The work had been done as an associated research work of LSRB-DRDO Sponsored project (GAP0623).

Conflict of interest

The authors declare that they have no conflict of interest.

References

1. Talebi S, Chaibakhsh N, Shoeili Z M (2017) Application of nanoscale ZnS/TiO_2 composite for optimized photocatalytic decolorization of a textile dye. J appl res tech 15: 378-385.
2. Ismail M, Akhtar K, Khan M I, Kamal T, Seo M A J, et al. (2019) Pollution, Toxicity And Carcinogenicity of organic dye Bio-Remediation. Current Pharmaceutical Design 25: 3653-3671.
3. Ahmad S, Khan SB, Asiri AM, Marwani HM, Kamal T (2020) Polypeptide and copper oxide nanocomposite hydrogel for toxicity elimination of wastewater. J Sci Tech 96: 382-394.
4. Katheresan V, Kansedo J, Lau SY (2018) Efficiency of various recent wastewater dye removal methods: A review. J Envir Chem Eng 6: 4676-4697.
5. Qin YL, Zhao WW, Sun Z, Liu XY, Shi GL, et al. (2018) Photocatalytic and adsorption property of Zn$STiO_2$/RGO ternary composites for methylene blue degradation. Ads sci tech 37: 764-776.
6. Anastasescua C, Negrilab C, Angelescua DG, Atkinsona I, Anastasescua M, et al. (2018) Particularities of photocatalysis and formation of reactive oxygen species on insulators and semiconductors: Cases of SiO_2, TiO_2 and their composite SiO_2-TiO_2. Catal Sci Technol 8: 5657-5668.
7. Nosaka Y, Nosaka AY (2017) Generation and Detection of Reactive Oxygen Species in Photocatalysis. Chem Rev 117: 11302–11336.
8. Wang R, Shi K, Huang D, Zhang J, An S (2019) Synthesis and degradation kinetics of TiO_2/GO composites with highly efficient activity for adsorption and photocatalytic degradation of MB. Scientific Reports 9: p18744.
9. Schrier J, Demchenko DO, Wang L (2007) Optical Properties Of Zno/Zns And Zno/Znte Heterostructures For Photovoltaic Applications. Nano Lett 7: 2377-2382.
10. Ranjith KS, Uyar T (2018) Conscientious design of zn-s/tin layer by transformation of $zntio_3$ on electrospun $zntio_3$@tio_2 nanofibers: Stability and reusable photocatalytic performance under visible irradiation. ACS Sustainable Chem Eng 6: 12980–12992.
11. Silva RD, Goncalves RH, Stroppa DG, Ramirezb AJ, Leite ER (2011) Synthesis of recrystallized anatase TiO_2 mesocrystals with wulff shape assisted by oriented attachment. Nanoscale 3: p1910.
12. Liu X, Gao Y, Cao C, Luo H, Wang W (2010) Highly crystalline spindle-shaped mesoporous anatase titania particles: Solution-Phase Synthesis, Characterization, and Photocatalytic Properties. Langmuir 26: 7671-7674.
13. Rahmawati F, Putri FR, Masykur A (2019) The Photocatalytic Activity Of Zns-Tio_2 On A Carbon Fiber Prepared By Chemical Bath Deposition. Open Chem 17: 132-141.
14. Stengl V, Bakardjieva S, Murafa N, Houskova V, Lang K (2007) Visible-light photocatalytic activity of TiO_2/ZnS nanocomposites prepared by homogeneous hydrolysis. Micro Meso Mat 110: 370–378.
15. Zhang L, Li Y, Wang M, Liu H, Chen H, et al. (2019) Construction of zns-in2s3 nanonests and its heterojunction boosted visible-light photocatalytic/photoelectrocatalytic performance. New J Chem 43: 14402-14408.
16. Lonkar SP, Pillai VV, Alhassan SM (2018) Facile and scalable production of heterostructured ZnS-ZnO/Graphene nano-photocatalysts for environmental remediation. Scientific Reports 8: p13401.
17. Boxi SS, Paria S (2014) Effect of silver doping on TiO_2, CdS, and ZnS nanoparticles for the photocatalytic degradation of metronidazole under visible light. RSC Adv 4: 37752-37760.
18. Xiaodan Y, Qingyin W, Shicheng J, Yihang G (2006) Nanoscale ZnS/TiO_2 composites: Preparation, characterization, and visible-light photocatalytic activity. Materials Characterization 57: 333-341.
19. Franco A, Neves MC, Ribeiro CMML, Mendonc MH, Pereiraa MI, et al. (2009) Photocatalytic decolorization of methylene blue in the presence of TiO_2/ZnS nanocomposites. J Hazar Mat 161: 545–550.
20. Stengl V, Kralova D (2011) Tio_2/zns/cds nanocomposite for hydrogen evolution and orange ii dye degradation. International J Phot 2011: 1-14.
21. Liang YC, Xu NC (2018) Synthesis of TiO_2ZnS nanocomposites via sacrificial template sulfidation and their ethanol gas-sensing performance. RSC Adv 8: p22437.
22. Harish S, Sabarinathan M, Periyanayaga AK, Archana J, Navaneethan M, et al. (2017) ZnS quantum dots impregnated-mesoporous TiO_2 nanospheres for enhanced visible light induced photocatalytic application. RSC Adv 7: 26446-26457.
23. Dahl M, Liu Y, Yin Y (2014) Composite titanium dioxide nanomaterials. Chem Rev 114: 9853–9889.
24. Kshirsagara AS, Khanna PK (2018) Titanium dioxide (tio_2) decorated silver indium diselenide (aginse2): Novel nano-photocatalyst for oxidative dye degradation. Inorganic chem front 5: 2242-2256.
25. Boulkroune R, Sebais M, Messai Y, Bourzami R, Schmutz M, et al. (2019) Hydrothermal synthesis of strontium-doped ZnS nanoparticles: Structural, electronic and photocatalytic investigations. Bull Mater Sci 42: p223.
26. Babu VJ, Vempati S, Ertas Y, Uyar T (2015) Excitation dependent recombination studies on SnO_2/TiO_2 electrospun nanofibers. RSC Adv 5: 66367-66375.
27. Prasannalakshmi P, Shanmugam N (2017) Fabrication of TiO_2/ZnS nanocomposites for solar energy mediated photocatalytic application. Spectrochimica Acta 175: 1-10.
28. Khan H, Samanta S, Seth M, Jana S (2020) Fabrication and photoelectrochemical activity of hierarchically Porous TiO_2ZnO heterojunction film. J Mater Sci 55: 11907-11918.
29. Rahmawati F, Wulandari R, Murni IM, Moedjijono M (2015) The optical properties and photo catalytic activity of zns-tio_2/graphite under ultra violet and visible light radiation. Bull Chem Reac Eng Cat 10: 294-303.
30. Liberto GD, Tosoni S, Pacchioni G (2016) Charge carriers cascade in a ternary tio_2/tio_2/zns heterojunction: A DFT study. ChemCatChem 12: 2097-2105.